Coupled acoustic/elastic wave propagation simulation using discontinuous Galerkin finite element method

H.Kamalinia, A.Barbarulo, B.Tie

Université Paris-Saclay, CentraleSupélec, CNRS, Laboratoire de Mécanique des Sols, Structures et Matériaux (MSSMat-UMR8579), 91190, Gif-sur-Yvette, France. email: bing.tie@centralesupelec.fr

Résumé — In this work, a discontinuous Galerkin (dG) finite element framework is introduced for the numerical simulation of the wave propagation in coupled acoustic/elastic media. A compact unified formulation is proposed for acoustic and elastic wave equations. Afterward, numerical fluxes on acoustic/elastic physical interfaces are developed by solving the exact Riemann problem. Finally, the coupled dG solver is verified by comparing the reflection and transmission coefficients to the analytical values, and is used to calculate the attenuation coefficient in the case of composite structures.

Mots clés — Discontinuous Galerkin method, wave propagation, acoustic/elastic coupling.

1 Introduction

The space discontinuous Galerkin (dG) finite element method is widely used for the numerical simulation of wave propagation in different media. Indeed, this method is easilly parallelizable thanks to its spatial element-wise discontinuous shape functions. Therefore, it provides an elegant framework to develop modern high-performance computing and to help overcome the challenge of computational cost in the case of complex media when the involved wavelengths are comparable or smaller than the characteristic lengths of the geometry. Furthermore, it is capable of combining the advantages of the finite element method in space with the high-order integration schemes.

Unlike the continuous finite element method, the dG method is based on the use of discontinuous basis functions between finite elements. However, this discontinuity must be controlled by defining appropriated numerical fluxes on the element interfaces. Hence, developing and implementing appropriate numerical fluxes is main key to success in the discontinuous Galerkin method. There is a large body of work focusing on the calculation of fluxes in pure elastic media [1, 2, 3, 4, 5, 6]. In the case of multiphysical couplings, there are several methods suggested in the literature for developing the numerical fluxes within the dG framework on the coupled interfaces, including the acoustic/elastic interface. Wilcox et al. [7] introduce a dG framework for isotropic elastic/acoustic using velocity-strain formulation by solving exact Riemann problem. Zhan et al. [8] also propose a velocity-strain discontinuous Galerkin in arbitrary anisotropic elastic/acoustic media by solving the exact Riemann problem. As an alternative way, the "penalty flux" method is used for calculation of the numerical flux, within both elastic velocity-strain [9] and elastic velocity-stress formulation[10].

In this work, which is based on the method and formulation proposed by Tie et al. [5, 6] for the elastic wave propagation in heterogeneous media, we introduce a coupled arbitrary anisotropic elastic/acoustic discontinuous Galerkin framework, in which the numerical fluxes are obtained by solving the exact Riemann problem on the interfaces. It is notheworthy that in our method, unlike the proposed framework in [7] and [8], we use the elastic velocity-stress and acoustic velocity-pressure formulations.

2 Acoustic and elastic wave propagation equations

Let's consider an acoustic or elastic n-dimension domain $\Omega \subset R^n$, in which the governing equations of either acoustic or elastic wave propagation is written in the form of a first-order hyperbolic system in space and time as follows : $\forall (\boldsymbol{x}, t) \in \Omega \times]0, T[$

$$\boldsymbol{M}(\partial_t \boldsymbol{U}) + \boldsymbol{A}^{\partial_x}(\boldsymbol{U}) = \boldsymbol{0} \tag{1}$$

The tensorial compact form (1) was proposed by Tie et al. in [5].

In the acoustic domain, the generalized unknown $U(x,t) = (v(x,t)\ p(x,t))^T$ is composed of v the velocity unknown and p the pressure one. Hence, $U(x,t)$ is a field in $\mathbb{R}^d \times \mathbb{R}$ and defined over the open set $\Omega \times]0,T[$. The operator M and the space derivative operator A^{∂_x} are defined as follows : $\forall W = (w\ q)^T$

$$M\begin{pmatrix} w \\ q \end{pmatrix} = \begin{pmatrix} \rho w \\ \lambda_f^{-1} q \end{pmatrix} \ , \ A^{\partial_x}\begin{pmatrix} w \\ q \end{pmatrix} = \begin{pmatrix} -\nabla_x q \\ -\operatorname{div}_x w \end{pmatrix} \tag{2}$$

where ρ and λ_f respectively denote the density and the bulk modulus of the fluid.

On the other hand, in the elastic domain, the operator M and space derivative operator A^{∂_x} are defined as follows : $\forall W = (w\ \tau)^T$

$$M\begin{pmatrix} w \\ \tau \end{pmatrix} = \begin{pmatrix} \rho w \\ C^{-1} : \tau \end{pmatrix} , \ A^{\partial_x}\begin{pmatrix} w \\ \tau \end{pmatrix} = \begin{pmatrix} -\mathbf{Div}_x\,\tau \\ -\varepsilon(w) \end{pmatrix} \tag{3}$$

where the generalized unknown $U(x,t) = (v(x,t)\ \sigma(x,t))^T$ is a field defined in $\mathbb{R}^d \times \mathbb{R}^{d \times d_{sym}}$ and is composed of the velocity v and the stress σ , and C is the fourth-order elasticity tensor.

It can be shown that on the boundary ∂D of any subdomain $D \subseteq \Omega$, the flux operator F_n (with $n = n_i e_i$ the outward unit normal vector defined on ∂D) associated to the first-order velocity-pressure system is equal to A_n, the Jacobian operator in the n direction. This, in the acoustic case, results in : $\forall W = (w\ q)^T$,

$$F_n(W) = A_n(W) = A_n\begin{pmatrix} w \\ q \end{pmatrix} = \begin{pmatrix} -qn \\ -n \cdot w \end{pmatrix} \tag{4}$$

and, in the elastic case, gives rise to : $\forall W = (w\ \tau)^T$,

$$F_n(W) = A_n\begin{pmatrix} w \\ \tau \end{pmatrix} = \begin{pmatrix} -\tau \cdot n \\ -n \otimes_s w \end{pmatrix} \tag{5}$$

Let's consider $\mathcal{M}_h = \{\Omega_k\}_k$ as a finite element mesh of the domain Ω. From now on, each element Ω_k of the mesh $\mathcal{M}_h$ will be denoted by E and any of its neighboring elements by E'. The space dG variational formulation of the coupled system (1) for any element E is written in the following form : $\forall W_h(x)$

$$(W_h, M(\partial_t U_h))_E - (W_h, A^{\partial_x}(U_h))_E + < W_h, \hat{F}_n(U_h, U_h') - F(U_h) >_{\partial E} = 0 \tag{6}$$

where $W_h(x) = (w_h(x)\ q_h(x))^T$ in the acoustic case, $W_h(x) = (w_h(x)\ \tau_h(x))^T$ in the elsatic case, U_h and U_h' are respectively the discontinuous solutions in E and E', and $\hat{F}_n(U_h, U_h')$ is the numerical flux which depends on the solution in both E and the adjacent element E'. The numerical flux in this paper is obtained by exact solving of the associated Riemann problem on the acoustic/acoustic, elastic/elastic and acoustic/elastic interfaces.

3 Riemann problem on the acoustic/elastic interface

In order to have the fully coupled solver, it is required to calculate the numerical flux on the elastic/elastic, acoustic/acoustic and acoustic/elastic interfaces. In this paper, we only mention the acoustic/elatic interface, since the elastic/elastic interface is explained in detail in [6], and the acoustic/acoustic interface is very straight forward which will be discussed in more detail in [11].

Before giving the definition of the Riemann problem on the interfaces, we recall the eigenvalues and eigenvectors of the acoustic and elastic first-order hyperbolic system (1). In both cases, the eigenvalues and eigenvectors are obtained by solving the following eigenproblem :

$$A_n(R_n) = \lambda_n M(R_n) \tag{7}$$

On the acoustic side, the solving of the eigenvalue problem (7) gives rise to $m = d+1$ eigenvalues $\{\lambda_{n,k}\}_{k=1,...m}$, two of which are non-zero. The two non-zero eigenvalues and the corresponding right eigenvectors $\{R_{n,k}\}_{k=1,...m}$ are as following :

$$\lambda_n^\pm = \pm\sqrt{\frac{\lambda_f}{\rho}} \ , \ R_n^\pm = \begin{pmatrix} \frac{1}{\sqrt{2}}n \\ -\frac{1}{\sqrt{2}}z_n^\pm \end{pmatrix} \tag{8}$$

where z_n is the acoustic impedance defined as : $z_n^{\pm} = \lambda_f(\lambda_n^{\pm})^{-1} = \rho\lambda_n^{\pm}$. Furthermore, it is easy to show that the left eigenvectors are :

$$L_n^{\pm} = \begin{pmatrix} \frac{1}{\sqrt{2}}n \\ -\frac{1}{\sqrt{2}}(z_n^{\pm})^{-1} \end{pmatrix} , \; M(R_n^{\pm}) = \rho L_n^{\pm} \tag{9}$$

On the elastic side, the charactristic structure of the first-order hyperbolic velocity-stress equation was studied in [6]. Among the $m = d + d(d+1)/2$ eigenvalues of A_n, there are d strictly negative eigenvalues $\lambda_{n,k}^{-}$ and d strictly positive eigenvalues $\lambda_{n,k}^{+}$. The right and left eigenmodes corresponding to the nonzero eigenvalues of A_n are the following : $\forall k = qL, \{qT_\alpha\}_{\alpha=1,\cdots,d-1}$

$$R_{n,k}^{\pm} = \begin{pmatrix} w_{n,k} \\ -\rho(z_{n,k}^{\pm})^{-1}C : (n \otimes_s w_{n,k}) \end{pmatrix} , \; L_{n,k}^{\pm} = \begin{pmatrix} w_{n,k} \\ -(z_{n,k}^{\pm})^{-1}n \otimes_s w_{n,k} \end{pmatrix} \tag{10}$$

with $w_{n,k} = \frac{1}{\sqrt{2}}\gamma_{n,k}$, $(\gamma_{n,k})_{k=qL,\{qT_\alpha\}_{\alpha=1,\cdots,d-1}}$ the unit eigenvectors of the following usual eigensystem of Γ_n the Christoffel tensor :

$$\Gamma_n \cdot \gamma_{n,k} = \lambda_{n,k}^2 \gamma_{n,k} \tag{11}$$

Now we consider the interface of two adjacent elements E and E', where the element E is governed by the acoustic wave equations with (ρ, λ_f, U_h) as density, bulk modulus and initial state, while E' is governed by the elastic wave equations with (ρ', C', U_h') as density, Hooke tensor and initial state (Figure 1). In this case, the Rankine-Hugoniot jump conditions are written as follows :
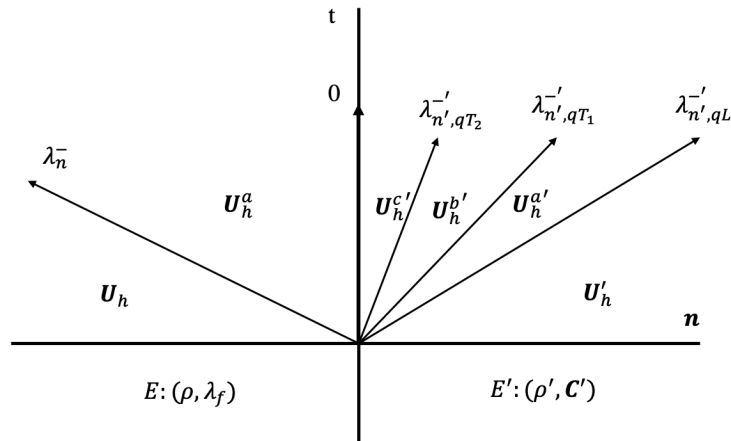

FIGURE 1 – Sketch illustration of the Rankine-Hugoniot jump condition in the Riemann problem for at the acoustic-elastic interface

$$A_n(U_h) - A_n(U_h^a) = \alpha\lambda_n^{-}M(R_n^{-}) \tag{12a}$$

$$A_n(U_h^a) + \Pi_n(A_{n'}'(U_h^{c'})) = 0 \tag{12b}$$

$$A_{n'}'(U_h') - A_{n'}'(U_h^{c'}) = \sum_{k=qL,qT_1,qT_2} \alpha_k'\lambda_{n',k}^{-}M'(R_{n',k}^{-}) \tag{12c}$$

where the operator $\Pi_n : \mathbb{R}^d \times \mathbb{R}^{d \times d_{sym}} \to \mathbb{R}^d \times \mathbb{R}$ is defined as :

$$\Pi_n(W) = \begin{pmatrix} w \\ (n \otimes n) : \tau \end{pmatrix} \tag{13}$$

We also need an operator $\Psi_n : \mathbb{R}^d \times \mathbb{R} \to \mathbb{R}^d \times \mathbb{R}^{d \times d_{sym}}$, which is in fact the adjoint operator of Π_n.

According to the definitions of A_n in both acoustic and elastic media and of Π_n, the equation (12b) gives rise to the following interface condition on the acoustic-elastic interface :

$$p_h^a n + \sigma_h^{c'} \cdot n' = 0 \; , \; n \cdot v_h^a + n' \cdot v_h^{c'} = 0 \tag{14}$$

Now, by eliminating the two unknown states U_h^a and $U_h^{c'}$ in (12), the characteristic coefficients $\{\alpha, \alpha_k'\}$ of the Riemann problem (12) are obtained by solving the following system of equations.

$$\begin{bmatrix} 1 & [B]_{1\times 3} \\ [B']_{3\times 1} & [Id]_{3\times 3} \end{bmatrix} \cdot \begin{pmatrix} \alpha \\ \{\alpha_k'\} \end{pmatrix} = \begin{bmatrix} \boldsymbol{L_n^-} \cdot (U_h - \boldsymbol{\Pi_{n'}}(U_h')) \\ 2\wp_{tens}(\boldsymbol{L_{n',k}^{-'}}) : \wp_{tens}(U_h' - \boldsymbol{\Psi_n}(U_h)) \end{bmatrix} \tag{15}$$

with :

$$B_{1l} = -\frac{z_{\boldsymbol{n}}^- - z_{\boldsymbol{n'},l}^{-'}}{2z_{\boldsymbol{n}}^-}(\boldsymbol{n} \cdot \boldsymbol{\gamma_{n',l}'}) \,, \; B_{l1}' = \frac{z_{\boldsymbol{n}}^-}{z_{\boldsymbol{n'},l}^{-'}}\boldsymbol{n} \cdot \boldsymbol{\gamma_{n',l}'} \tag{16}$$

and $\wp_{tens}(\cdot)$ is an operator that gives the tensorial component when it is applied to the generalized vector $\boldsymbol{W} = (\boldsymbol{w} \; \boldsymbol{\tau})^T$. After solving the system of equations (15) for characteristic equations, the numerical flux on the acoustic/elastic interface is calculated using the following equation :

$$\hat{\boldsymbol{F}}_{\boldsymbol{n}}(U_h, U_h') = \boldsymbol{A_n}(U_h) - \alpha\lambda_{\boldsymbol{n}}^- M(\boldsymbol{R_n^-}) \tag{17}$$

4   Numerical Results : validation and application

The first objective here is validating the proposed dG method and the numerical fluxes and showing the accuracy of the computed results. For this purpose, the numerically obtained reflection and transmission coefficients are compared to the analytical values. Afterward, a more complicated example with multiple circular acoustic/elastic interfaces is considered, which is addressed more in detail in section 4.2.

4.1   Analytical/numerical comparison

In this section, a rectangular domain is considered with an acoustic subdomain Ω_1 and an elastic subdomain Ω_2, as it can be illustrated in Figure 2. In this example, the physical parameters are as following :

$$\rho_1 = 1000 \; kg/m^3, \quad c = 1500 \; m/s \;\; (x,y) \in \Omega_1 \tag{18a}$$
$$\rho_2 = 4000 \; kg/m^3, \quad c_p = 3000 \; m/s \;\; (x,y) \in \Omega_2 \tag{18b}$$
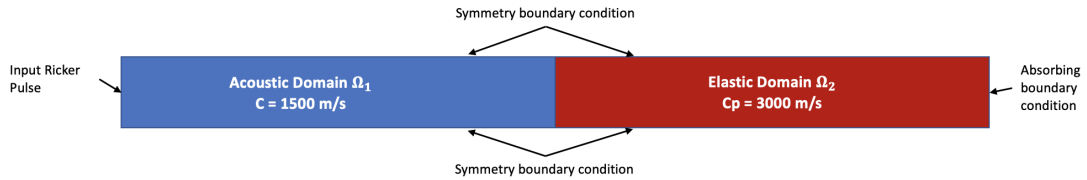

FIGURE 2 – Considered geometry for calculation of the numerical reflection and transmission coefficeints

As it is illustrated in Figure 2, the input pulse is placed on the left, and we consider symmetry boundary condition on the top and bottom edge, and absorbing boundary condition on the right. By imposing this set of boundary conditions of the geometry, we will only observe the propagation of the P-wave inside the elastic domain.

The input pulse is a Ricker wavelet with the maximum frequency of $f_{max} = 10 \; KHz$ and the cutoff frequency of $f_c = 34 \; KHz$. The size of the element in this example is estimated by placing 20 elements per smallest wavelength (the wavelength associated with the cutoff frequency). In addition, since space dG solver is an explicit solver, it is necessary to calculate the appropriate time step in order to avoid instability. It was observed that CFL=0.2 will guarantee the stability of the solver.

Figure 3a shows the incident and reflected signals recorded at a point in the center of the acoustic subdomain. In addition, Figure 3b illustrates the transmitted signal at the center point of the elastic subdomain. The value of the numerical reflection and transmission coefficients are calculated respectively by dividing the maximum amplitude of the reflected and transmitted signals respectively by the maximum amplitude of the incident signal. Table 1 presents the value of the numerical and analytical reflection and transmission coefficients.
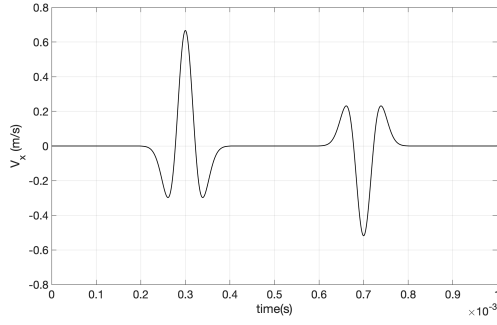
(a) The incident and reflected Ricker wavelet in the acoustic subdomain
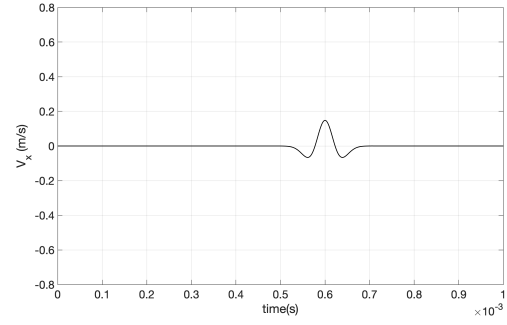
(b) The transmitted Ricker wavelet in the elastic subdomain

FIGURE 3 – The velocity signal on the center point of each subdomains

TABLE 1 – Calculated analytical and numerical reflection and transmission coefficents

	Analytical	Numerical	Error %
Reflection Coefficent	0.7778	0.7773	0.06
Transmission Coefficent	0.2222	0.2220	0.09

4.2 Calculation of the attenuation coefficient

The objective of this section is to study the wave propagation in the nearly incompressible materials in which the propagation speed of the S-wave is negligible compared to the propagation speed of the P-wave. For that purpose, a sandwich composite structure occupying a rectangular 2D domain and composed of a matrix, circular inclusions, and a rigid shell surrounding the matrix is studied. In this considered configuration, the matrix (Ω_1) is made of an incompressible solid material, such as an elastomer, and inclusions (Ω_2) and the surrounding shell (Ω_3) are made of a hard polymer.

The physical parameters of the matrix are as following :

$$\rho_1 = 1000 \, kg/m^3, \qquad c_{p_1} = 1620 \, m/s, \ c_{s_1} = 16 m/s \ \ (x,y) \in \Omega_1 \tag{19}$$

In this example, the effect of the material properties of the inclusions and the surrounding shell on the attenuation coefficient is investigated for a distribution of the inclusions inside the matrix, the Ricker wavelet with $f_{max} = 5 \, MHz$ and $f_c = 17 \, MHz$ is initiated on the top boundary, the symmetry boundary condition is placed on the right and left sides, and the bottom boundary is free. The receiver is also placed over the top boundary, to record the signal. The propagation speed of the P-wave is changed from 2700 m/s to 1700 m/s, and the attenuation coefficient is calculated using the following equation :

$$\alpha = -\frac{5}{D} ln \frac{\Sigma_{j=1}^{j=M} A^r(x_j)}{\Sigma_{j=1}^{j=M} A^{Ref}(x_j)} \tag{20}$$

where D is the traveled distance, M is the number of points on the receiver, A^r is the reflected signal, and A^{Ref} is the reference signal which in this case is the incident wave.

For these examples, two scenarios are considered : First, the elastic dG method is used for modeling the wave propagation in the incompressible matrix, and afterward, the acoustic solver is used for the matrix.

Figure 4a shows the average velocity signal over 100 points on the receiver, for the case in which the propagation speed of the P-wave inside the inclusions is $2740m/s$. This figure shows that at the beginning, the obtained signals from two solvers are identical (before $t = 1.1\mu s$), containing the incident and first reflection from the interface between the shell and the matrix. In addition, the reflected signal from the bottom boundary, which is used for the calculation of the attenuation coefficient, are almost identical as well, using both elastic and acoustic/elastic solvers. By plotting the attenuation coefficient with respect to the ratio of the acoustic impedances of the inclusions and the matrix (Figure 4b), we observe that the difference is negligible. In this curve (Figure 4b), moving to the right side of the x-axis
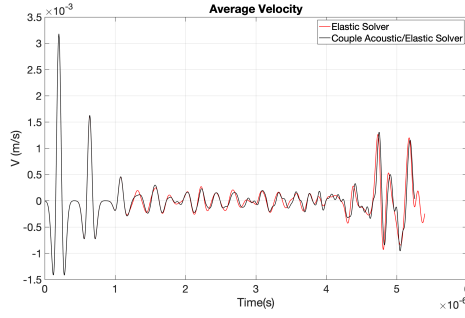
(a) Average velocity signal recorded on the top boundary : $cp_2 = 2740$ in Ω_2 and Ω_3
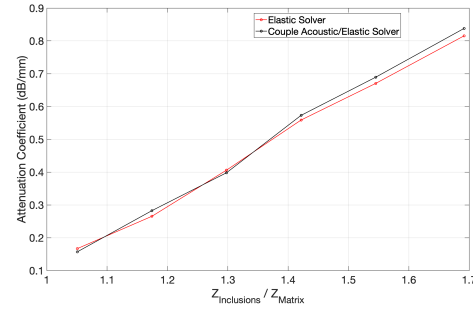
(b) Attenuation coefficient with respect to ratio of acoustic Impedances

FIGURE 4 – Comparing the results obtained from pure Elastic and coupled Acoustic/Elastic solver

basically means that the material used as the inclusion is stiffer, or in another word, has a larger value of Young's modulus.

Since the total number of degrees of freedom is smaller by using the acoustic solver (3 degrees of freedom per node instead of 5), and solving the Riemann problem on the coupled interface has no extra complexity for the solver to deal with, we decrease the calculation cost using the coupled acoustic/elastic solver. Hence, we showed that in this particular example, the same value of a attenuation coefficient could be obtained with less calculation cost, thanks to the coupled acoustic/elastic solver.

5 Conclusions

A compact intrinsic variational framework of discontinuous Galerkin method for coupled acoustic/elastic wave propagation was presented in multidimensional case and for a general Hooke tensor on the elastic side. The upwind numerical flux on the element interfaces was calculated by solving the exact corresponding Riemann problem. The treatment of the acoustic/elastic physical interfaces are especially studied. In order to validate the solver and the proposed numerical flux and to show their accuracy, the numerical reflection and coefficients obtained for a simple rectangular domain with an acoustic/elastic interface are compared to the analytical values, the relative error is less than 0.1%. Afterward, a more complicated example with circular acoustic/elastic interface. In this case the coupled discontinuous Galerking solver is working perfectly. It was also shown that for some particular applications such as nearly incompressible materials and for a target parameter such as attenuation coefficient, the acoustic solver could replace the elastic solver, to reduce the calculation cost of the simulation. Indeed, it was observed by using the coupled acoustic/elastic solver instead of the pure elastic solver for a nearly incompressible material in a sandwich composite structure, the same values of attenuation coefficient is obtained by using the less expensive acoustic/elastic solver.

Acknowledgments

Références

[1] Bernardo Cockburn, George E. Karniadakis, and Chi-Wang Shu, editors. *Discontinuous Galerkin Methods : Theory, Computation and Applications*. Lecture Notes in Computational Science and Engineering. Springer-Verlag, Berlin Heidelberg, 2000.

[2] Martin Käser and Michael Dumbser. An arbitrary high-order discontinuous Galerkin method for elastic waves on unstructured meshes - I. The two-dimensional isotropic case with external source terms. *Geophysical Journal International*, 166(2) :855–877, August 2006.

[3] Michael Dumbser and Martin Käser. An arbitrary high-order discontinuous Galerkin method for elastic waves on unstructured meshes - II. The three-dimensional isotropic case. *Geophysical Journal International*, 167(1) :319–336, October 2006.

[4] Josep de la Puente, Martin Käser, Michael Dumbser, and Heiner Igel. An arbitrary high-order discontinuous Galerkin method for elastic waves on unstructured meshes - IV. Anisotropy. *Geophysical Journal International*, 169(3) :1210–1228, June 2007.

[5] Bing Tie, Anne-Sophie Mouronval, Van-Dang Nguyen, Laurent Series, and Denis Aubry. A unified variational framework for the space discontinuous Galerkin method for elastic wave propagation in anisotropic and piecewise homogeneous media. *Computer Methods in Applied Mechanics and Engineering*, 338 :299–332, August 2018.

[6] Bing Tie and Anne-Sophie Mouronval. Systematic development of upwind numerical fluxes for the space discontinuous Galerkin method applied to elastic wave propagation in anisotropic and heterogeneous media with physical interfaces. *Computer Methods in Applied Mechanics and Engineering*, 372 :113352, December 2020.

[7] Lucas C. Wilcox, Georg Stadler, Carsten Burstedde, and Omar Ghattas. A high-order discontinuous Galerkin method for wave propagation through coupled elastic–acoustic media. *Journal of Computational Physics*, 229(24) :9373–9396, December 2010.

[8] Qiwei Zhan, Qiang Ren, Mingwei Zhuang, Qingtao Sun, and Qing Huo Liu. An exact Riemann solver for wave propagation in arbitrary anisotropic elastic media with fluid coupling. *Computer Methods in Applied Mechanics and Engineering*, 329 :24–39, February 2018.

[9] Ruichao Ye, Maarten V. de Hoop, Christopher L. Petrovitch, Laura J. Pyrak-Nolte, and Lucas C. Wilcox. A discontinuous Galerkin method with a modified penalty flux for the propagation and scattering of acousto-elastic waves. *Geophysical Journal International*, 205(2) :1267–1289, May 2016.

[10] Kaihang Guo, Sebastian Acosta, and Jesse Chan. A weight-adjusted discontinuous Galerkin method for wave propagation in coupled elastic-acoustic media. *Journal of Computational Physics*, 418 :109632, October 2020.

[11] Hossein Kamalinia, Andrea Barbarulo, and Bing Tie. Development of upwind numerical fluxes for the space discontinuous galerkin method in the coupled acoustic-elastic wave propagation simulation. *To be submitted*, 2022.